Importance of elastic finite-size effects: Neutral defects in ionic compounds

P. A. Burr*
School of Electrical Engineering and Telecommunications, University of New South Wales, Kensington, 2052 New South Wales, Australia

M. W. D. Cooper
Materials Science and Technology Division, Los Alamos National Laboratory, P.O. Box 1663, Los Alamos, New Mexico 87545, USA
(Received 20 March 2017; revised manuscript received 11 May 2017; published 15 September 2017)

Small system sizes are a well-known source of error in density functional theory (DFT) calculations, yet computational constraints frequently dictate the use of small supercells, often as small as 96 atoms in oxides and compound semiconductors. In ionic compounds, electrostatic finite-size effects have been well characterized, but self-interaction of charge-neutral defects is often discounted or assumed to follow an asymptotic behavior and thus easily corrected with linear elastic theory. Here we show that elastic effects are also important in the description of defects in ionic compounds and can lead to qualitatively incorrect conclusions if inadequately small supercells are used; moreover, the spurious self-interaction does not follow the behavior predicted by linear elastic theory. Considering the exemplar cases of metal oxides with fluorite structure, we show that numerous previous studies, employing 96-atom supercells, misidentify the ground-state structure of (charge-neutral) Schottky defects. We show that the error is eliminated by employing larger cells (324, 768, and 1500 atoms), and careful analysis determines that elastic, not electrostatic, effects are responsible. The spurious self-interaction was also observed in nonoxide ionic compounds irrespective of the computational method used, thereby resolving long-standing discrepancies between DFT and force-field methods, previously attributed to the level of theory. The surprising magnitude of the elastic effects is a cautionary tale for defect calculations in ionic materials, particularly when employing computationally expensive methods (e.g., hybrid functionals) or when modeling large defect clusters. We propose two computationally practicable methods to test the magnitude of the elastic self-interaction in any ionic system. In commonly studied oxides, where electrostatic effects would be expected to be dominant, it is the elastic effects that dictate the need for larger supercells: greater than 96 atoms.

DOI: 10.1103/PhysRevB.96.094107

I. INTRODUCTION

Finite-size effects have been a known limitation since the beginning of atomic-scale simulations of solids [1,2]. These arise when atomic interactions extend beyond the simulation boundaries. Most modern atomic-scale simulation methods adopt periodic boundary conditions (PBCs) to represent crystalline matter and introduce defects through the use of supercells [3]. Of primary concern for finite-size effects are long-range interactions through elastic (strain) fields and electrostatic (Coulomb) fields. Elastic self-interactions of point defects have been studied since the early days of atomic-scale simulations, first for simple elemental metals [4–7] and later for ionic crystals [3,8]. This was dictated by necessity, as the existing computational resources limited the size of force-field simulations to tens of atoms: now 10^{12} atoms can be modeled [9]. While the computational power available to atomic scale modelers has increased dramatically, the typical simulation size used for density functional theory (DFT) calculations has not increased accordingly, in favor of ever-increasing sophistication in the description of the electronic state. However, much of the old knowledge regarding the importance of accounting for elastic self-interactions seems to be lost or ignored in many recent reports.

In ionic materials, where, typically, point defects are charged, Coulomb interactions are assumed to be predominant. Consequently, a large body of research has focused on predicting and countering the electrostatic self-interaction energy in DFT, producing a number of charge correction schemes with increasing degrees of complexity and sophistication [10–17]. On the other hand, elastic self-interactions, which are thoroughly accounted for in metals and ionocovalent materials [2,3,18,19], have largely been neglected in strongly ionic compounds, being perceived to be of secondary importance to electrostatic interactions. Here we show that for charge-neutral defects, the elastic interactions are non-negligible and lead to a qualitative change in defect stability.

We consider exemplar cases of metal oxides with fluorite structure (CeO_2, ThO_2, UO_2, and actinide oxides) that have been extensively studied in the past due to their engineering applications, including solid oxide fuel cells (SOFCs), electrolyzer cells, ion conductors, catalysts, and nuclear fuel. Specifically, we consider the formation of charge-neutral Schottky clusters $\{V_O^{\cdot\cdot} : V_M^{////} : V_O^{\cdot\cdot}\}^{\times}$, which are known to reduce oxygen mobility [20–23], degrade the electrolytic properties of SOFCs [23–25], and govern the distribution and retention of gaseous fission products in nuclear fuel [26–30]. We also extend the study to nonoxide ionic compounds with fluorite structure (CaF_2) and antifluorite structure (Be_2C, also ionic [31,32]) to show that the phenomenon is not limited to oxides.

The formation and migration of charge-neutral clusters in these metal oxides has been extensively investigated with *ab initio* simulations [23,24,30,33–49], but nearly all of the studies were carried out with simulation cells containing up to 96 atoms ($2 \times 2 \times 2$ supercell), with a few instances where larger supercells were used [48,50–52]. Of the three possible

*p.burr@unsw.edu.au

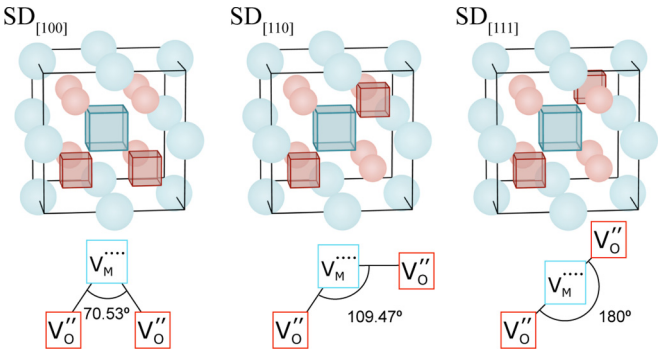

FIG. 1. Three possible configurations of the bound SD in the fluorite structure, defined by the arrangement of the anion vacancies around the cation vacancy.

configurations that a bound Schottky defect (SD) may exhibit (see Fig. 1), the DFT studies consistently report the $SD_{[110]}$ configuration as the lowest-energy cluster. One exception is the publication by Yu *et al.* [53]; however, their reported Schottky energies appear to be orders of magnitude smaller than those in all other published work. On the other hand, modeling studies employing empirical force fields, and thus frequently using very large periodic simulations cells or the Mott-Littleton approach [54], often report the inverse: that $SD_{[111]}$ is more favorable than $SD_{[110]}$ [55–57], although there is large variation in results as the quality of the potentials precludes the apparent stability of Schottky clusters. It is unclear to what extent the discrepancy between empirical and *ab initio* results is due to the different level of theory (DFT vs force fields) or to finite-size effects. In this paper we show that DFT and reliable force-field potentials are, indeed, in agreement if the results are compared across the same supercell sizes. Notably, two studies employed $3 \times 3 \times 3$ supercell (324 atoms) of ThO_2 [51,52]. Murphy *et al.* [52] reported similar trends between DFT and force-field simulations for increasing supercell size; however, the discrepancy regarding the most favorable cluster configuration still remained. Although their subject does not belong to the family of fluorite compounds, Bradley *et al.* [50] also employed a 324-atom supercell of m-HfO_2 to study defect clusters.

In this paper, we show that charge-neutral Schottky clusters interact over long ranges through elastic fields and that the commonly used 96-atom supercell is inadequately small to capture the correct ground state of Schottky clusters. We then show that the root cause of this finite-size effect is spurious interaction between strain fields across PBCs and not electrostatic or electronic effects. Additionally, the elastic finite-size effect is not described accurately by linear elastic theory, owing to the complex mode of relaxation. We conclude by proposing two methods to estimate, albeit approximately, the magnitude of the elastic self-interaction for any ionic system.

II. METHODOLOGY

Force-field simulations were performed with the LAMMPS code [58,59], using the many-body potential of Cooper, Rushton, and Grimes (CRG) [57], as this potential set proved to be reliable and transferable [60–64] across a wide range of MO_2 compounds. DFT simulations were carried out with VASP [65], using the Perdew-Burke-Ernzerhof (PBE) exchange-correlation functional [66], projector augmented-wave pseudopotentials with the maximum number of valence electrons available [67], and a plane-wave cutoff of 500 eV. Details of the k-point grids and evidence of convergence to within 1 meV are provided in the Supplemental Material [68]. c-ZrO_2 was also initially investigated, but due to the stability of m-ZrO_2 it was not possible to retain the cubic symmetry during relaxation of defects in large cells, even by constraining some degrees of freedom.

On-site Coulomb correction terms have been included for CeO_2 and UO_2, following the majority of the published studies [42–48,69–76]: Dudarev *et al.*'s formalism [77] for CeO_2 with $U\{Ce_{4f}\} = 5.0$ eV, $U\{O_{2p}\} = 5.5$ eV, and Liechtenstein *et al.*'s formalism [78] for UO_2 with $U\{U_{5f}\} = 4.5$ eV and $J\{U_{5f}\} = 0.51$ eV. U ramping [79] (for CeO_2) and occupation matrix control [69,73] (for UO_2) were used to avoid metastable states. Details are provided in the Supplemental Material [68] together with results obtained without U to emphasize that the findings are not sensitive to the choice of simulation parameters. UO_2 was described with collinear 1**k** antiferromagnetic ordering, as this is the best collinear approximation of the true (noncollinear 3**k** antiferromagnetic [80,81]) magnetic ordering of UO_2 [44–48,71–73].

In ionic materials, the formation energy of a defect d with charge q is conventionally calculated as

$$E_d^f = E_{\text{def}} - E_{\text{perf}} \pm \sum_\alpha n_\alpha \mu_\alpha - q\mu_e + E_{\text{chcor}} + E_{\text{elcorr}}, \quad (1)$$

where E_{def} and E_{perf} are the DFT total energies of the defective and pristine supercells, respectively, μ_α is the chemical potential of all species added or removed to form the defect, μ_e is the Fermi level of the system with respect to the valence-band maximum, E_{chcorr} is a charge correction term, following a number of possible schemes [10–17], and E_{elcorr} is the energy due to elastic self-interaction, seldom accounted for in ionic compounds. Since (a) the defects considered here are charge neutral, (b) the composition of the defects is precisely one stoichiometric formula unit (i.e., $\mu_{MO_2} = \frac{E_{\text{perf}}}{x}$, where x is the number of formula units in the supercell), and (c) the elastic self-interaction is the subject of the study, the defect formation energy of a Schottky cluster is simplified to

$$E_{\text{SD}}^f = E_{\text{def}} - E_{\text{perf}} - \frac{E_{\text{perf}}}{x}, \quad (2)$$

$$E_{\text{SD}}^f = E(M_{x-1}O_{2x-2}) - \frac{x-1}{x} E(M_xO_{2x}), \quad (3)$$

in line with previous publications [43–45]. This simplification conveniently removes any dependence of our results on external factors such as the chemical potential of reference elements or the apparent band gap of the material.

The linear elastic theory approximation to E_{elcorr} was calculated with the aid of the ANETO script [18] from the stress tensor of the relaxed simulations and using elastic constants obtained from DFT simulations through lattice perturbation to retain self-consistency. Selected calculations were repeated where atomic relaxation was restricted to atoms within a

relaxation radius from the defect center, and all other atoms were kept fixed at the perfect lattice site.

III. RESULTS AND DISCUSSION

The effect of finite PBCs was first investigated using the CRG potential. Figure 2 shows the formation energy (solid symbols) of bound Schottky clusters in various actinide oxides and CeO_2. It is clear that, irrespective of the cation species, the $SD_{[111]}$ defect is the most favorable when simulated in large enough supercells (containing 324 atoms or more), but $SD_{[110]}$ is the most favorable in the smaller simulation cell containing 96 atoms. The results of calculations before geometry relaxation are also presented in the top panel, showing no crossover of defect energies.

To show that the crossover was not a peculiarity of the CRG potential form, DFT calculations were performed with supercells containing 96, 324, and 768 atoms on selected oxides (CeO_2, ThO_2, UO_2) as well as CaF_2 and Be_2C (Fig. 3). Be_2C has a very small lattice parameter; therefore a further supercell containing 1500 atoms was also considered. It is evident that DFT and force-field calculations are in agreement, and crossover between $SD_{[111]}$ and $SD_{[110]}$ occurs between the $\sim$10 Å supercells (96 atoms) and the $\sim$16 Å supercells (324 atoms). The trend is predicted for CaF_2 and Be_2C as well as the oxides. Importantly, including the energy penalty predicted from linear elastic theory (dashed lines) does not correct the trend.

It is well known that point defects in ionic materials interact chiefly though their charges, and although the Schottky clusters have no overall charge, they still comprise three charge defects ($V^{2-}_{\text{anion}} - V^{4+}_{\text{cation}} - V^{2-}_{\text{anion}}$) that may individually interact across periodic boundaries. In addition, $SD_{[100]}$ and $SD_{[110]}$ also exhibit effective dipoles since the geometrical center of the positive charges does not align with that of the negative charges. $SD_{[111]}$ does not have an associated dipole since it is a linear defect with mirror symmetry. Nevertheless, to show that electrostatic interactions alone cannot account for this peculiar finite-size effect, all charge-charge, charge-dipole, and dipole-dipole interactions have been evaluated independently (Fig. 4). Three point charges (two positive and one negative with no overall charge) were arranged in a dielectric medium with the same configurations as the three bound Schottky defects and then replicated in a repeating array of $10 \times 10 \times 10$ to model the effect of PBCs, where the distance between replicas was increased progressively to simulate larger supercells. Dielectric constants, the lattice parameter, and the magnitude of charges are arbitrary. However, a range of $\frac{q^2}{\varepsilon a}$ ratios have been modeled, all yielding the same qualitative behavior.

Figure 4 shows that as the supercell size increases, the energy contribution from self-interaction across periodic boundaries tend to zero (see insets); therefore the total energy of each system converges toward the internal energy of the point-charge triplet, consisting entirely of Coulomb interactions. It is clear that the three point-charge configurations (representative of the three Schottky clusters) never cross over at any separation; hence the electrostatic interactions alone do not account for the change in relative stability of Schottky clusters. This is reassuring, given that CaF_2 shows trend similar to CeO_2, ThO_2, and UO_2 despite a factor of $\frac{1}{2}$ difference in ionic charges (Fig. 3).

Beyond electrostatic effects, electronic effects may also lead to a change in behavior with increasing supercell size. This has been well documented for charge-neutral vacancies in Si [82–84], where small simulation cells (64 atoms or fewer) predict a retention of T_d symmetry, while larger cells correctly identify a reduction of local symmetry to D_{2d}, as observed experimentally. The symmetry reduction and associated energy reduction are due to a Jahn-Teller distortion [85], and consequently, the effect is strongly sensitive to Brillouin zone sampling as well as supercell size [83]. SiC is another example of a covalent material where similar effects have been observed [86]. Jahn-Teller effects are not limited to covalently

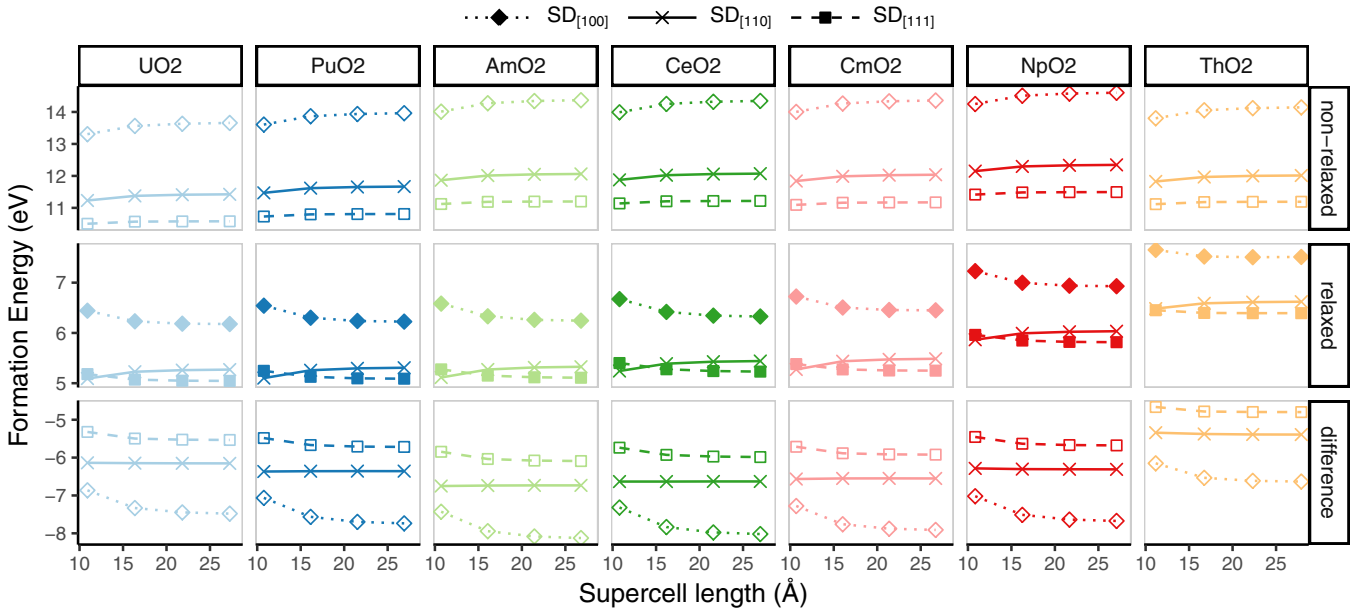

FIG. 2. Defect formation energy (before and after relaxation) from CRG potentials versus supercell size (from $2 \times 2 \times 2$ to $5 \times 5 \times 5$) for three bound Schottky configurations in actinide oxides and CeO_2. Values for ThO_2 were taken from [52].

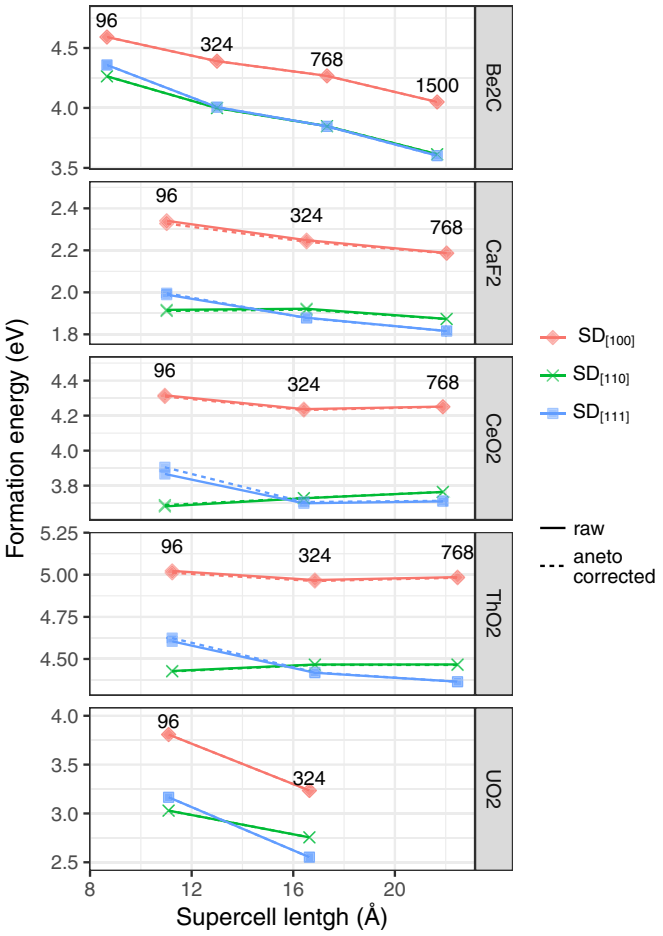

FIG. 3. Defect formation energies from DFT as a function of supercell size (labels indicate atoms in the supercell). UO_2 simulations were limited to 324 atoms due to the additional complexity and computational cost of OMC.

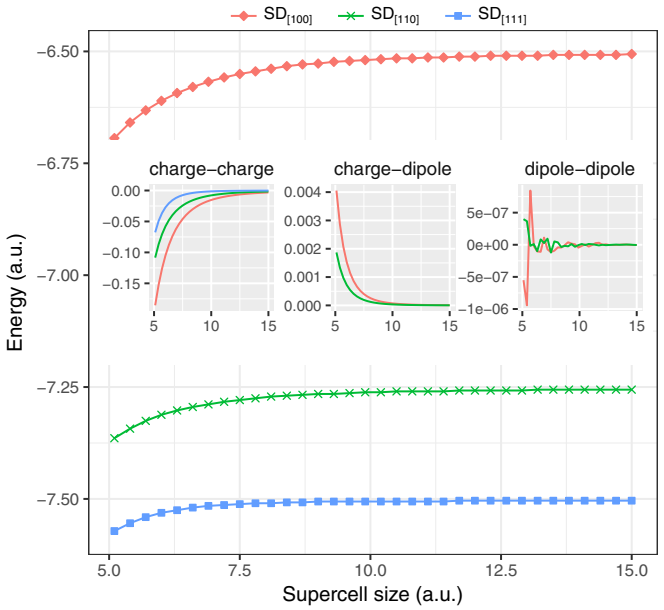

FIG. 4. Total electrostatic energy of SD modeled as point charges arranged in a dielectric medium with periodic boundaries. Inset: energy contribution from self-interaction across supercell boundaries.

bonded materials; in fact they are known to be important in many oxides [73,87]. However, the finite-size effect observed in the current study was consistently reproduced with the generalized gradient approximation (GGA), GGA + U and force-field potentials (with fixed charges on atoms), suggesting that electronic effects cannot be at the heart of the matter.

The source of the crossover is instead found in the elastic interactions. Figure 2 shows that prior to geometry relaxation there is no crossover in stability between $SD_{[110]}$ and $SD_{[111]}$. This is also shown for DFT calculations in the Supplemental Material [68]. Thus relaxation is hampered in the smallest supercell. Figure 5 depicts the atomic displacements caused by the three bound Schottky clusters in the largest DFT cell of CeO_2. The boundaries of the smaller supercells are superimposed on the image to highlight that the strain field exceeds the bounds of the $2 \times 2 \times 2$ supercell (96 atoms). The displacement fields are better quantified in Fig. 6, where the atomic displacements are plotted as a function of distance from the cation vacancy. The atomic displacements obtained from the largest supercell reveal that at a distance of 7 Å from V_{Ce}'''' (i.e., between the $2 \times 2 \times 2$ and $3 \times 3 \times 3$ boundaries) O atoms are displaced by as much as 11.5 pm, which is not insignificant. More importantly, when comparing the atomic displacements within the first 10 Å across different supercell sizes, it is evident that the fingerprint of atomic relaxation in the 96-atom supercell is fundamentally different from that of the larger supercells; that is, not only the magnitude but also the *shape* of the strain field is different. On the other hand, the fingerprint of atomic displacements changes only marginally when increasing supercell size further.

The fact that the shape of the displacement fields is fundamentally different between the 96-atom supercell and the larger supercells indicates that atomic relaxation is hampered by artificial restoring forces stemming from the PBCs. This frustration of atomic relaxation can provide only a positive contribution to the total energy of the system.

Generally, it is possible to predict the energy contribution arising from elastic self-interaction through methods based on linear elastic theory, which combine the elastic dipole tensor of the simulation with the elastic constants of the material [3,18]. However, Fig. 3 shows that the ANETO correction, which has been proven successful in a variety of metallic and covalent systems [18,88–92], cannot counter the finite-size effects observed here.

The inability of linear elastic theory to predict the energy contribution in ionic compounds is attributed to the complex relaxation pattern caused by the defect. Figure 5 clearly shows that the pattern of atomic displacements is not consistent with a simple compression (acoustic) wave, where all atoms move coherently towards the vacancies to accommodate the defect volume. The relaxation field more closely resembles that of an optical mode, where anions and cations exhibit distinct and more complex displacement patterns. This is evidenced more clearly in Fig. 7, where the radial component of the displacement vector is compared against that of an isostructural metallic compound (Al_2Au). In the metallic compound, the atomic relaxations are nearly exclusively towards the vacancy cluster (negative radial displacements), and the effect diminishes nearly monotonically with distance. In the

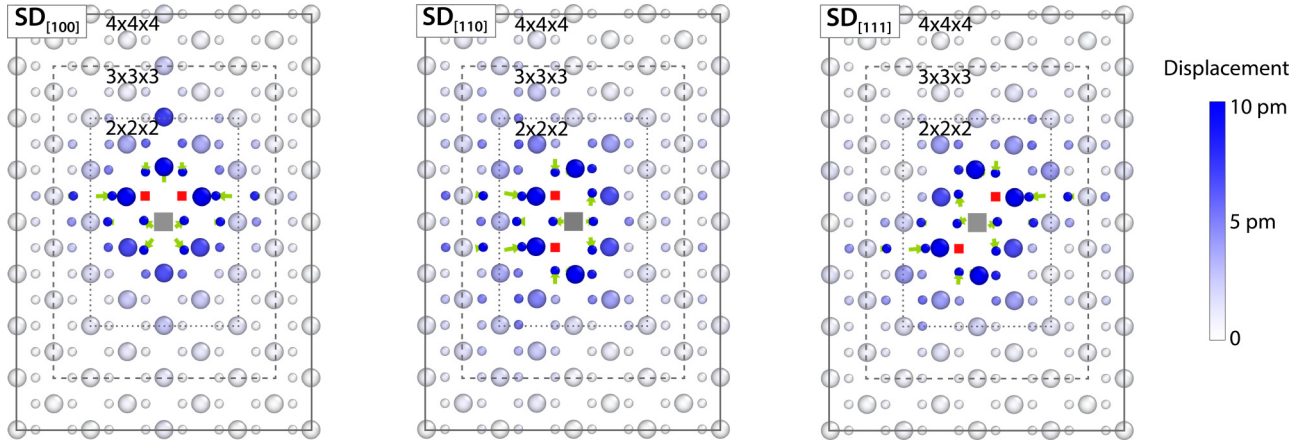

FIG. 5. The (110) slice (three atomic layers) of the 768-atom supercell of CeO_2. Dashed lines represent the boundaries of the smaller supercells. Gray and red squares represent the Ce and O vacancies, respectively; the green arrows represent the displacement magnitude scaled up by a factor of 5. First-nearest-neighbor atoms exceed the color map with displacements of up to 26 pm.

ionic compound, each shell of anions and cations exhibits both inward and outward displacements (with the exception of the first oxygen shell). As with any optical mode, this behavior may arise only in compound materials, explaining why it has not been observed in well-studied elemental materials. In addition, Fig. 7 shows that the phenomenon is restricted to ionic compounds, where alternating shells of anions and cations move in opposite directions in response to displacement of charge (e.g., neighboring ions).

The spurious interaction results in a change in shape of relaxation near the defect core, which cannot be captured by the dipole tensor: the dipole tensor may be obtained (a) from the (anisotropic) stress tensor and/or strain tensors on the cell or (b) by convergent summation of atomic displacements and/or restoring forces on atoms [93]. In both cases the dipole tensor may capture only a truncation of the strain field and not a change in shape of the core of the field (i.e., the "optical relaxation"), which is illustrated particularly clearly in Fig. 6 by comparison between the $2 \times 2 \times 2$ and $3 \times 3 \times 3$ supercells for which there is a notable change in relaxation displacements for atoms even within 5 Å of the defect. These core atoms are $<6-10$ Å away from the defect replica in the $2 \times 2 \times 2$ supercell.

As further evidence that the source of the self-interaction energy is the inhibition of elastic relaxation, we have performed calculations where only atoms within a given radius of the defect center were allowed to relax while all other

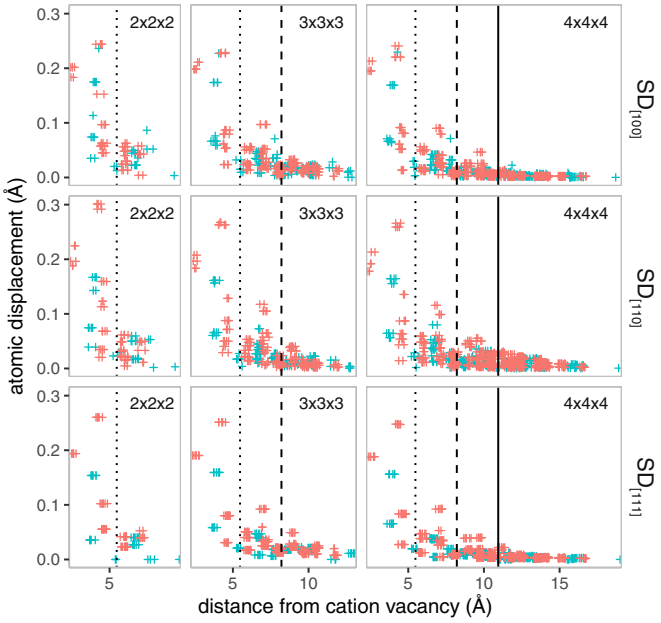

FIG. 6. Atomic displacements caused by Schottky clusters in CeO_2 supercells. Red and turquoise crosses represent O and Ce atoms, respectively. Black vertical lines represent half of the supercell length, following the same key as in Fig. 5. Beyond those lines, some atoms are closer to the periodic replica of the defect than the central defect.

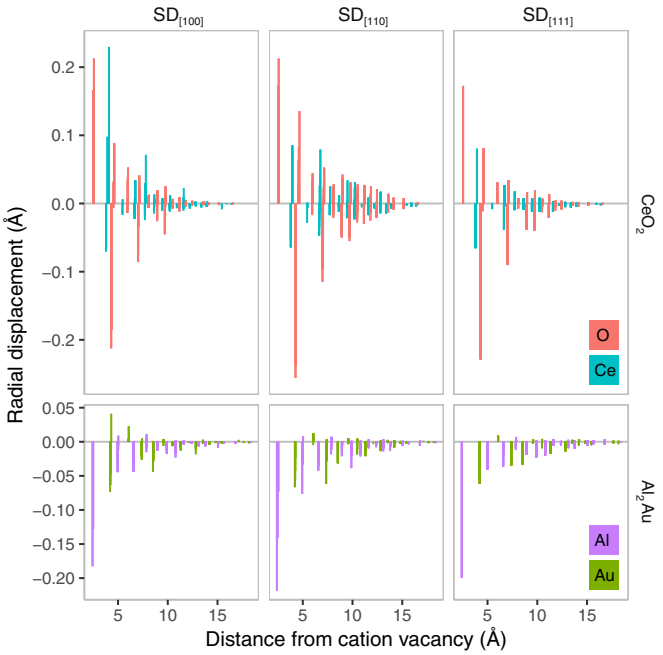

FIG. 7. Radial displacement d_r caused by Schottky clusters in CeO_2 and Al_2Au. $d_r = \boldsymbol{d} \cdot \boldsymbol{r}$, where $\boldsymbol{d}$ is the displacement vector and $\boldsymbol{r}$ is the position vector with respect to the cation vacancy.

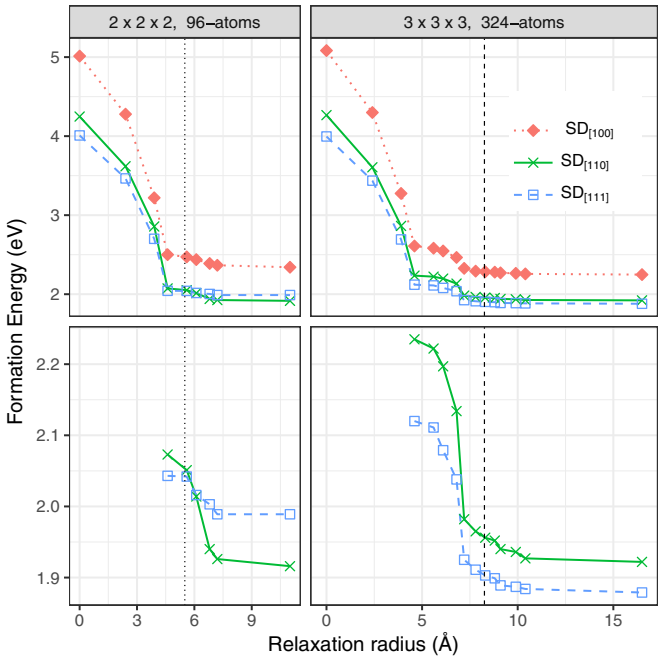

FIG. 8. Formation energies of Schottky defects in CaF_2 as a function of relaxation radius, whereby all atoms beyond that radius are forcefully kept fixed in their perfect lattice sites. Bottom panels provide an enlarged view of the crossover region. The vertical black line represents the largest radius that may be accommodated in the supercell without overlap ($R_{\text{relax}} = \frac{L}{2}$). The first and last points in each plot represent a single-point calculation and a complete relaxation, respectively.

atoms were "clamped" at perfect lattice positions (see Fig. 8). Provided that the relaxation radius is less than half the supercell length, $R_{\text{relax}} = \frac{L}{2}$, this constraint ensures that no strain is transmitted across the PBCs. Thus the relaxation field, although artificially truncated at the given radius, is entirely due to the defect and not its periodic replicas.

When the relaxation radius is less than half the supercell length (i.e., the region of atoms that are allowed to relax fits entirely within the supercell), $SD_{[110]}$ appears less favorable than $SD_{[111]}$, consistent with the findings obtained from very large supercell simulations. Only when the relaxation radius is larger than half the cell length (i.e., atoms within the sphere respond to the strain field of the defect *and* its replicas) does the apparent crossover in stability manifest in the 96-atom supercell. This is a further confirmation that the phenomenon is due to the interaction of strain fields across PBCs in the smaller supercells.

Constraining atomic positions as a function of distance from the defect allows one to isolate the relaxation strain component of the defect energy. By iterating that procedure over increasing relaxation radii, it is evident that the behavior is distinctly not monotonic, with two clear steps at the fourth and eighth nearest neighbors. This is at odds with the behavior expected from a continuum elastic medium.

It is concluded that if inadequately small supercells are used, 96 atoms or less for fluorite structure oxides, the spurious self-interaction is beyond the reach of linear elastic theory and thus cannot be corrected for without further calculations. It is not always possible to increase the simulation size, especially when performing calculations with computationally expensive methods, such as hybrid functionals, *ab initio* molecular dynamics, or time-dependent DFT. Thus here we propose two computationally practicable methods to ascertain whether finite-size effects are significant in the system of interest:

(1) One option is to use a lower level of theory method to perform the convergence test. In the current work, we have shown that CRG force-field potential was as predictive as DFT in the analysis of the spurious self-interaction. Thus, if reliable force-field potentials are available for the system of interest, these may be used to test supercell convergence. Similarly, for hybrid calculations, one could use local-density approximation or GGA functionals to test the supercell size convergence. Note, however, that this is a two-stage approach: in the first instance one must test that within the same supercell size the two methods yield similar trends. Quantitative agreement is not expected, but any qualitative agreement between the two methods observed in the small simulation size is expected to be preserved in larger simulations cells (as shown in the current work). Note that this method cannot be extended to electronic self-interaction, as these are highly sensitive to the description of the electronic states [84].

(2) The alternative approach is to use a range-dependent constraint method with $R_{\text{relax}} = \frac{L_{\text{min}}}{2}$, as illustrated in Fig. 8, to test whether there is qualitative agreement between the fully relaxed simulations and those where the strain fields were not allowed to transfer across the PBCs. Incidentally, this method also significantly reduces the computational cost of energy minimization because of the reduced internal degrees of freedom. The size of the discrepancy may be considered as an indicator of the extent to which strain extends beyond the PBCs.

IV. CONCLUSIONS

Electrostatic self-interactions have long been thought to be the dominant source of finite-size effects in ionic materials. Here we have shown that even in ionic compounds, elastic self-interactions are non-negligible, causing qualitative and quantitative changes to the energy and structure of defects. This finite-size effect is the source of numerous inaccurate reports in the *ab initio* literature regarding the defect stability of many important functional oxides, including CeO_2, ThO_2, and UO_2. The magnitude of the elastic self-interaction is such that it warrants the need for simulations sizes larger than the widely used 96-atom supercell for cubic oxide compounds. In addition, we show that the spurious self-interaction cannot be countered by simple linear elastic theory approaches.

We considered the exemplar cases of charge-neutral Schottky clusters in fluorite-structured oxides and performed DFT and force-field simulations in supercells of increasing size up to 1500 atoms. Supercells of 96 atoms were not sufficiently large to capture the most stable neutral Schottky clusters compared to larger cells. This behavior was observed also for nonoxide ionic compounds with related structures (prototypical fluorite CaF_2 and antifluorite Be_2C) but was not observed in isostructural metallic compounds. This phenomenon is also insensitive to the level of theory used (force field embedded atom model, DFT, DFT + U).

We provided evidence that the finite-size effect is not due to electrostatic self-interaction (accounting for charge-charge, charge-dipole, and dipole-dipole interactions) or electronic effects (owing to the presence of the self-interaction in force-field calculations with fixed charges); instead, it is caused by spurious interaction of strain fields across PBCs. This was confirmed through the use of range constraints, where selected atoms were fixed to the perfect lattice sites, thereby artificially truncating the strain field before the PBCs. In these simulations the correct order of defect energies was restored. Surprisingly, the spurious self-interaction energy cannot be accounted for by, and therefore corrected with, linear elastic theory. The failure of linear elastic theory is attributed, through careful analysis of the displacement fields, to the complex relaxation patterns observed in the ionic compounds, akin to optical modes.

Our findings also resolve a long-standing discrepancy between DFT and force-field simulations regarding the ground state of neutral defect clusters in actinide oxides. This had typically been attributed to the simplified atomic interactions of the empirical force-field methods, but we showed that good agreement is, in fact, obtained when comparing across the same supercell sizes. The fact that the phenomenon is observed at all levels of theory can be exploited to the practitioners' advantage, using computationally simpler methods to test the degree of elastic self-interaction in the system of interest.

Although we have focused primarily on bound Schottky defects, the findings are likely relevant to other neutral clusters and their migration pathways, such as $\{2Y'_{Zr} : V_O^{\cdot\cdot}\}^{\times}$ and $\{2Gd'_{Ce} : V_O^{\cdot\cdot}\}^{\times}$ in yttria-stabilized zirconia and gadolinia-doped ceria. Rather than just being considered a spurious size effect for dilute limit calculations, the elastic effects discussed here also apply to real materials with high concentrations of Schottky defects, providing an insight into the interaction between two or more Schottky clusters that come within 10–16 Å of each other. This may be an important factor in the nucleation of voids in nuclear fuels and SOCFs.

The current work should serve as a cautionary tale for future simulations of all ionic systems, especially those where computational requirements dictate the use of small supercell sizes. While proving that 96-atom supercells are inadequate for point defect analysis in fluorite-structured oxides, every solid-state system would have different supercell requirements. In the current paper we provided two computationally efficient methods to ascertain whether elastic finite-size effects are significant for the system of interest: (1) comparison with a lower level of theory (as exemplified here using force-field CRG potentials) and (2) comparison with range-constrained simulations (where selected atoms have been fixed to the perfect lattice sites to hamper propagation of strain fields).

ACKNOWLEDGMENTS

The authors would like to acknowledge S. T. Murphy, N. Kuganathan, M. J. D. Rushton, and R. W. Grimes for the useful discussions. M.W.D.C. is funded by the U.S. Department of Energy, Office of Nuclear Energy, Nuclear Energy Advanced Modeling Simulation (NEAMS) program. Los Alamos National Laboratory, an affirmative action/equal opportunity employer, is operated by Los Alamos National Security, LLC, for the National Nuclear Security Administration of the US Department of Energy under Contract No. DE-AC52- 06NA25396. P.A.B. acknowledges the Australian Nuclear Science and Technology Organisation and the A. W. Tyree Foundation for their charitable financial support. Computational resources were provided by the National Computational Infrastructure (NCI), which is supported by the Australian Government, and the Multi-modal Australian ScienceS Imaging and Visualisation Environment (MASSIVE) (www.massive.org.au), though the national merit allocation scheme (NCMAS) and UNSW's "HCP@NCI" trial scheme.

[1] *Computer Simulation of Solids*, edited by C. R. A. Catlow and W. C. Mackrodt (Springer-Verlag, Berlin, Heidelberg, 1982).
[2] C. Freysoldt, B. Grabowski, T. Hickel, J. Neugebauer, G. Kresse, A. Janotti, and C. G. Van De Walle, Rev. Mod. Phys. **86**, 253 (2014).
[3] M. Leslie and M. J. Gillan, J. Phys. C **18**, 973 (1985).
[4] J. Eshelby, Acta Metall. **3**, 487 (1955).
[5] J. R. Hardy and R. Bullough, Philos. Mag. **15**, 237 (1967).
[6] B. K. D. Gairola, Phys. Status Solidi B **85**, 577 (1978).
[7] J. R. Hardy, J. Phys. Chem. Solids **29**, 2009 (1968).
[8] M. J. Gillan, J. Phys. C **17**, 1473 (1984).
[9] W. Eckhardt, A. Heinecke, R. Bader, M. Brehm, N. Hammer, H. Huber, H.-G. Kleinhenz, J. Vrabec, H. Hasse, M. Horsch, M. Bernreuther, C. W. Glass, C. Niethammer, A. Bode, and H.-J. Bungartz, in *Supercomputing: 28th International Supercomputing Conference, ISC 2013, Leipzig, Germany, June 16–20, 2013, Proceedings*, edited by J. M. Kunkel, T. Ludwig, and H. W. Meuer (Springer, Berlin, 2013), pp. 1–12.
[10] G. Makov and M. C. Payne, Phys. Rev. B **51**, 4014 (1995).
[11] S. Lany and A. Zunger, Modell. Simul. Mater. Sci. Eng. **17**, 084002 (2009).
[12] C. Freysoldt, J. Neugebauer, and C. G. Van de Walle, Phys. Rev. Lett. **102**, 016402 (2009).
[13] N. D. M. Hine, K. Frensch, W. M. C. Foulkes, and M. W. Finnis, Phys. Rev. B **79**, 024112 (2009).
[14] C. Freysoldt, J. Neugebauer, and C. G. Van de Walle, Phys. Status Solidi B **248**, 1067 (2011).
[15] S. E. Taylor and F. Bruneval, Phys. Rev. B **84**, 075155 (2011).
[16] S. T. Murphy and N. D. M. Hine, Phys. Rev. B **87**, 094111 (2013).
[17] Y. Kumagai and F. Oba, Phys. Rev. B **89**, 195205 (2014).
[18] C. Varvenne, F. Bruneval, M.-C. Marinica, and E. Clouet, Phys. Rev. B **88**, 134102 (2013).
[19] S. K. Jain, V. Juričić, and G. T. Barkema, Phys. Rev. B **94**, 020102 (2016).
[20] A. R. Genreith-Schriever, P. Hebbeker, J. Hinterberg, T. Zacherle, and R. A. De Souza, J. Phys. Chem. C **119**, 28269 (2015).
[21] M. O. Zacate, L. Minervini, D. J. Bradfield, R. W. Grimes, and K. E. Sickafus, Solid State Ionics **128**, 243 (2000).
[22] S. Grieshammer, B. O. H. Grope, J. Koettgen, and M. Martin, Phys. Chem. Chem. Phys. **16**, 9974 (2014).

[23] S. Grieshammer, M. Nakayama, and M. Martin, Phys. Chem. Chem. Phys. **18**, 3804 (2016).

[24] Z. P. Li, T. Mori, F. Ye, D. R. Ou, J. Zou, and J. Drennan, Phys. Rev. B **84**, 180201 (2011).

[25] Y.-M. Kim, J. He, M. D. Biegalski, H. Ambaye, V. Lauter, H. M. Christen, S. T. Pantelides, S. J. Pennycook, S. V. Kalinin, and A. Y. Borisevich, Nat. Mater. **11**, 888 (2012).

[26] A. Chroneos, Appl. Phys. Rev. **3**, 041304 (2016).

[27] M. Bertolus, M. Freyss, B. Dorado, G. Martin, K. Hoang, S. Maillard, R. Skorek, P. Garcia, C. Valot, A. Chartier, L. Van Brutzel, P. Fossati, R. W. Grimes, D. C. Parfitt, C. L. Bishop, S. T. Murphy, M. J. Rushton, D. Staicu, E. Yakub, S. Nichenko, M. Krack, F. Devynck, R. Ngayam-Happy, K. Govers, C. S. Deo, and R. K. Behera, J. Nucl. Mater. **462**, 475 (2015).

[28] T. Ichinomiya, B. P. Uberuaga, K. E. Sickafus, Y. Nishiura, M. Itakura, Y. Chen, Y. Kaneta, and M. Kinoshita, J. Nucl. Mater. **384**, 315 (2009).

[29] M. W. D. Cooper, S. C. Middleburgh, and R. W. Grimes, Solid State Ionics **266**, 68 (2014).

[30] X. Y. Liu, D. A. Andersson, and B. P. Uberuaga, J. Mater. Sci. **47**, 7367 (2012).

[31] P. Herzig and J. Redinger, J. Chem. Phys. **82**, 372 (1985).

[32] C.-T. Tzeng, K.-D. Tsuei, and W.-S. Lo, Phys. Rev. B **58**, 6837 (1998).

[33] K. Shao, H. Han, W. Zhang, H. Wang, C.-Y. Wang, Y.-L. Guo, C.-L. Ren, and P. Huai, J. Nucl. Mater. **490**, 181 (2017).

[34] G. E. Murgida, V. Ferrari, M. V. Ganduglia-Pirovano, and A. M. Llois, Phys. Rev. B **90**, 115120 (2014).

[35] B. Wang, X. Xi, and A. N. Cormack, Chem. Mater. **26**, 3687 (2014).

[36] T. Zacherle, A. Schriever, R. A. De Souza, and M. Martin, Phys. Rev. B **87**, 134104 (2013).

[37] P. R. L. Keating, D. O. Scanlon, and G. W. Watson, J. Mater. Chem. C **1**, 1093 (2013).

[38] X. Y. Liu and K. E. Sickafus, J. Nucl. Mater. **414**, 217 (2011).

[39] M. Nakayama and M. Martin, Phys. Chem. Chem. Phys. **11**, 3241 (2009).

[40] H. Y. Xiao, Y. Zhang, and W. J. Weber, J. Nucl. Mater. **414**, 464 (2011).

[41] F. Gupta, A. Pasturel, and G. Brillant, J. Nucl. Mater. **385**, 368 (2009).

[42] P. R. L. Keating, D. O. Scanlon, B. J. Morgan, N. M. Galea, and G. W. Watson, J. Phys. Chem. C **116**, 2443 (2012).

[43] A. E. Thompson and C. Wolverton, Phys. Rev. B **84**, 134111 (2011).

[44] J.-P. Crocombette, Phys. Rev. B **85**, 144101 (2012).

[45] J.-P. Crocombette, D. Torumba, and A. Chartier, Phys. Rev. B **83**, 184107 (2011).

[46] B. Dorado, M. Freyss, B. Amadon, M. Bertolus, G. Jomard, and P. Garcia, J. Phys. Condens. Matter **25**, 333201 (2013).

[47] H. Y. Geng, Y. Chen, Y. Kaneta, M. Iwasawa, T. Ohnuma, and M. Kinoshita, Phys. Rev. B **77**, 104120 (2008).

[48] E. Vathonne, J. Wiktor, M. Freyss, G. Jomard, and M. Bertolus, J. Phys. Condens. Matter **26**, 325501 (2014).

[49] B. Huang, Philos. Mag. **94**, 3052 (2014).

[50] S. R. Bradley, G. Bersuker, and A. L. Shluger, J. Phys. Condens. Matter **27**, 415401 (2015).

[51] N. Kuganathan, P. S. Ghosh, C. O. T. Galvin, A. K. Arya, B. K. Dutta, G. K. Dey, and R. W. Grimes, J. Nucl. Mater. **485**, 47 (2017).

[52] S. T. Murphy, M. W. D. Cooper, and R. W. Grimes, Solid State Ionics **267**, 80 (2014).

[53] J. Yu, R. Devanathan, and W. J. Weber, J. Phys. Condens. Matter **21**, 435401 (2009).

[54] N. F. Mott and M. J. Littleton, Trans. Faraday Soc. **34**, 485 (1938).

[55] K. Govers, S. Lemehov, M. Hou, and M. Verwerft, J. Nucl. Mater. **366**, 161 (2007).

[56] D. S. Aidhy, P. C. Millett, T. Desai, D. Wolf, and S. R. Phillpot, Phys. Rev. B **80**, 104107 (2009).

[57] M. Cooper, M. Rushton, and R. Grimes, J. Phys. Condens. Matter **26**, 105401 (2014).

[58] S. Plimpton, LAMMPS molecular mechanics code, http://lammps.sandia.gov

[59] S. Plimpton, J. Comput. Phys. **117**, 1 (1995).

[60] P. S. Ghosh, N. Kuganathan, C. O. T. Galvin, A. Arya, G. K. Dey, B. K. Dutta, and R. W. Grimes, J. Nucl. Mater. **479**, 112 (2016).

[61] X.-Y. Liu, M. W. D. Cooper, K. J. McClellan, J. C. Lashley, D. D. Byler, B. D. C. Bell, R. W. Grimes, C. R. Stanek, and D. A. Andersson, Phys. Rev. Appl. **6**, 044015 (2016).

[62] M. W. D. Cooper, N. Kuganathan, P. A. Burr, M. J. D. Rushton, R. W. Grimes, C. R. Stanek, and D. A. Andersson, J. Phys. Condens. Matter **28**, 405401 (2016).

[63] F. Yuan, Y. Zhang, and W. J. Weber, J. Phys. Chem. C **119**, 13153 (2015).

[64] M. Rushton and A. Chroneos, Sci. Rep. **4**, 6068 (2014).

[65] G. Kresse and J. Furthmüller, Phys. Rev. B **54**, 11169 (1996).

[66] J. P. Perdew, K. Burke, and M. Ernzerhof, Phys. Rev. Lett. **77**, 3865 (1996).

[67] G. Kresse and D. Joubert, Phys. Rev. B **59**, 1758 (1999).

[68] See Supplemental Material at http://link.aps.org/supplemental/10.1103/PhysRevB.96.094107 for details of the computational method and defect energy of unrelaxed DFT calculations.

[69] J. P. Allen and G. W. Watson, Phys. Chem. Chem. Phys. **16**, 21016 (2014).

[70] D. A. Andersson, S. I. Simak, B. Johansson, I. A. Abrikosov, and N. V. Skorodumova, Phys. Rev. B **75**, 035109 (2007).

[71] J. Wiktor, G. Jomard, M. Torrent, and M. Bertolus, J. Phys. Condens. Matter **29**, 035503 (2017).

[72] B. Dorado and P. Garcia, Phys. Rev. B **87**, 195139 (2013).

[73] B. Dorado, G. Jomard, M. Freyss, and M. Bertolus, Phys. Rev. B **82**, 035114 (2010).

[74] M. Iwasawa, Y. Chen, Y. Kaneta, T. Ohnuma, H.-Y. Geng, and M. Kinoshita, Mater. Trans. **47**, 2651 (2006).

[75] A. Kotani and T. Yamazaki, Prog. Theor. Phys. Suppl. **108**, 117 (1992).

[76] T. Yamazaki and A. Kotani, J. Phys. Soc. Jpn. **60**, 49 (1991).

[77] S. L. Dudarev, G. A. Botton, S. Y. Savrasov, C. J. Humphreys, and A. P. Sutton, Phys. Rev. B **57**, 1505 (1998).

[78] A. I. Liechtenstein, V. I. Anisimov, and J. Zaanen, Phys. Rev. B **52**, R5467 (1995).

[79] B. Meredig, A. Thompson, H. A. Hansen, C. Wolverton, and A. van de Walle, Phys. Rev. B **82**, 195128 (2010).

[80] L. Desgranges, Y. Ma, P. Garcia, G. Baldinozzi, D. Siméone, and H. E. Fischer, Inorg. Chem. **56**, 321 (2017).

[81] K. Ikushima, S. Tsutsui, Y. Haga, H. Yasuoka, R. E. Walstedt, N. M. Masaki, A. Nakamura, S. Nasu, and Y. Onuski, Phys. Rev. B **63**, 104404 (2001).

[82] J. L. Mercer, J. S. Nelson, A. F. Wright, and E. B. Stechel, Modell. Simul. Mater. Sci. Eng. **6**, 1 (1998).
[83] M. J. Puska, S. Pöykkö, M. Pesola, and R. M. Nieminen, Phys. Rev. B **58**, 1318 (1998).
[84] S. A. Centoni, B. Sadigh, G. H. Gilmer, T. J. Lenosky, T. Díaz de la Rubia, and C. B. Musgrave, Phys. Rev. B **72**, 195206 (2005).
[85] H. A. Jahn and E. Teller, Proc. R. Soc. London, Ser. A **161**, 220 (1937).
[86] A. Zywietz, J. Furthmüller, and F. Bechstedt, Phys. Rev. B **59**, 15166 (1999).
[87] I. S. Elfimov, V. I. Anisimov, and G. A. Sawatzky, Phys. Rev. Lett. **82**, 4264 (1999).
[88] P. A. Burr, M. Wenman, B. Gault, M. P. Moody, M. Ivermark, M. J. D. Rushton, M. Preuss, L. Edwards, and R. W. Grimes, J. Nucl. Mater. **467**, 320 (2015).
[89] R. Agarwal and D. R. Trinkle, Phys. Rev. B **94**, 054106 (2016).
[90] T. Garnier, Z. Li, M. Nastar, P. Bellon, and D. R. Trinkle, Phys. Rev. B **90**, 184301 (2014).
[91] D. Murali, M. Posselt, and M. Schiwarth, Phys. Rev. B **92**, 064103 (2015).
[92] C. Varvenne, O. Mackain, and E. Clouet, Acta Mater. **78**, 65 (2014).
[93] R. Nazarov, J. S. Majevadia, M. Patel, M. R. Wenman, D. S. Balint, J. Neugebauer, and A. P. Sutton, Phys. Rev. B **94**, 241112 (2016).